DOI 10.1007/s11182-019-01603-4

Russian Physics Journal, Vol. 61, No. 10, February, 2019 (Russian Original No. 10, October, 2018)

STUDY OF PECULIARITIES OF THE MICROWAVE ABSORPTION SPECTRUM OF NANOCRYSTALLINE THIN MAGNETIC FILMS

B. A. Belyaev,[1,2] N. M. Boev,[1,2] A. V. Izotov,[1,2] and P. N. Solovev[1,2] UDC 537.621; 004.942

Based on the micromagnetic model which takes into account the random distribution of the uniaxial magnetic anisotropy directions in crystallites of a nanocrystalline film, an effective method has been implemented for calculation of the magnetization dynamics in microwave fields. For a certain range of crystallite sizes, when the energy of the random magnetic anisotropy is comparable to the exchange energy, a significant change of the ferromagnetic resonance field, broadening of the resonance line, and the appearance of an asymmetry in the shape of the resonance curve were found. With an increase of the crystallite sizes, the resonance field first grows, then, it quickly decreases to its minimum, and then, it grows again to reach saturation. In this case, the steepness of the left slope of the broadening resonance curve first decreases faster than that of the right slope, leading to the symmetry breaking of the resonance curve shape, then, the curve becomes symmetrical again, and then, the steepness of the left slope becomes greater than that of the right slope.

Keywords: micromagnetic modeling, nanocrystallites, random magnetic anisotropy, ferromagnetic resonance, microwave.

INTRODUCTION

Soft magnetic nanocrystalline materials are the object of increased interest among researchers due to the unique magnetic and electrical properties that distinguish them favorably from polycrystalline materials and even single crystals. As a rule, nanocrystalline alloys have a higher electrical resistivity, and therefore, a greater thickness of the skin layer at high frequencies. But the main advantages of the nanocrystalline alloys are the higher values of the saturation magnetization and high-frequency magnetic permeability [1, 2], which allows to use these materials in microwave devices.

Thin films and multilayer structures of nanocrystalline magnetic materials are of particular interest for applications: they can be used as controlled media in microwave devices developed on the principles of integrated planar technology. In particular, thin magnetic films (TMFs) with uniaxial magnetic anisotropy are used as sensitive elements in sensors of weak magnetic fields designed on the resonant microstrip structures [3, 4]. The possibility to vary the saturation magnetization and the value of the uniaxial magnetic anisotropy of TMF by changing the composition and technological fabrication conditions allows changing the magnetic permeability and the upper boundary of the operating frequency band over a wide range [5]. The relationship between the magnetic permeability and the frequency of ferromagnetic resonance (FMR) for thin films, called Acher's law [5, 6], shows a clear advantage of planar magnetic materials compared to the bulk ones.

One of the most important results obtained in the course of studying the nanocrystalline thin films was the experimental detection of complicated dependences of the magnetic microstructure, anisotropy, coercive force, and

[1]Kirensky Institute of Physics, Federal Research Center KSC of the Siberian Branch of the Russian Academy of Sciences, Krasnoyarsk, Russia, e-mail: belyaev@iph.krasn.ru; iztv@mail.ru; [2]Siberian Federal University, Krasnoyarsk, Russia, e-mail: nik88@inbox.ru; solap@ya.ru. Translated from Izvestiya Vysshikh Uchebnykh Zavedenii, Fizika, No. 10, pp. 50–56, October, 2018. Original article submitted August 27, 2018.

permeability of the magnetic medium on the crystallite (grain) size D [7]. If the crystallite size exceeds the exchange correlation radius, then, the magnetization vector is oriented along the easy anisotropy axis of the corresponding crystallite. With a decrease in the crystallite size, the energy of the exchange interaction between the crystallites gradually becomes greater than the anisotropy energy. Therefore, the magnetic moments of the adjacent grains tend to align parallel to each other. In this case, a peculiar magnetic structure arises with spatial deviations of magnetic moments from a certain mean direction called in the literature the magnetization ripple. With a further decrease in the grain size, the amplitude of these deviations decreases and the nanocrystalline film becomes uniformly magnetized.

The purpose of this work is to study the effect of the crystallite size D on the FMR in nanocrystalline thin films. For this purpose, a micromagnetic model of the nanocrystalline TMF was developed and an effective method for calculating its microwave absorption spectrum was implemented. A systematic numerical analysis of the TMF model was carried out, which made it possible to establish a number of features related to the effect of D on the substantial shift of the resonance field, as well as on the broadening of the FMR line and the appearance of a resonance curve asymmetry.

1. MODEL OF NANOCRYSTALLINE TMF AND METHOD FOR CALCULATING THE MAGNETIZATION DYNAMICS

To study properties of nanocrystalline thin magnetic films, we use the following expression for the free energy F:

$$F = \int_V \left[-\boldsymbol{H}\cdot\boldsymbol{M} + \frac{A}{M_s^2}\left(\nabla \boldsymbol{M}\right)^2 - \frac{1}{2}\boldsymbol{H}^m\cdot\boldsymbol{M} - \frac{K_u}{M_s^2}\left(\boldsymbol{M}\cdot\boldsymbol{n}\right)^2 - \frac{K}{M_s^2}\left(\boldsymbol{M}\cdot\boldsymbol{l}\right)^2 \right] dV\,. \tag{1}$$

Here, the first term describes the energy of an external magnetic field H (Zeeman energy), the second one describes the exchange interaction energy with the exchange stiffness constant A, the third term describes the energy of the demagnetizing field $\boldsymbol{H}^m$, and the fourth term describes the energy of the overall for the film uniaxial magnetic anisotropy with a constant K_u and an easy axis unit vector $\boldsymbol{n}$. The last term of the expression describes the energy of the uniaxial magnetic anisotropy K with a random direction of the easy magnetization axes in crystallites described by the unit vector $\boldsymbol{l} = \boldsymbol{l}(\boldsymbol{r})$. The distribution of the magnetization is characterized by the vector $\boldsymbol{M}(\boldsymbol{r})$, whose modulus is a constant $|\boldsymbol{M}(\boldsymbol{r})| = M_s$.

When the model is discretized by the finite-difference method, TMF is divided into N identical discrete cells in the form of a parallelepiped with the volume V_0 and magnetization vectors $\boldsymbol{M}_i$, (i = 1, 2, ..., N), constant within each cell. In this case, expression (1) for the free energy can be written as [8]

$$F = -V_0 \sum_{i=1}^{N} \left[\boldsymbol{H}_i \boldsymbol{M}_i + \frac{1}{2}\sum_{j=1}^{N} \boldsymbol{M}_i G_{ij} \boldsymbol{M}_j \right], \tag{2}$$

where G_{ij} is the 3×3 tensor describing the interaction between i and j discrete elements. The tensor G_{ij} does not depend on the direction of the magnetization $\boldsymbol{M}_i$ and is determined only by the internal properties of the magnetic system under study. The tensor G_{ij} is determined by the sum of tensors of the exchange interaction G_{ij}^e and magnetostatic interaction G_{ij}^m, and also tensors G_{ij}^u and G_{ij}^a describing the common for the entire film and random uniaxial magnetic anisotropy, respectively. The elements of the symmetric tensors describing the exchange interaction and magnetic anisotropy are defined as

$$G_{ij}^e = \frac{2J}{M_s^2}E \ \text{(for neighboring } i \text{ and } j\text{)},\ G_{ij}^u = \frac{2K_{ui}}{M_s^2}\boldsymbol{n}_i \otimes \boldsymbol{n}_j \delta_{ij}\,,\ G_{ij}^a = \frac{2K_i}{M_s^2}\boldsymbol{l}_i \otimes \boldsymbol{l}_j \delta_{ij}\,, \tag{3}$$

where $J = A/d^2$ and d is the distance between the adjacent discrete elements, E is the 3×3 identity matrix, the sign $\otimes$ denotes the tensor product, and δ_{ij} is the Kronecker symbol. To calculate the components of the magnetostatic interaction tensor G_{ij}^m, one usually uses either an approximation based on the allowance for the interaction of a pair of point magnetic dipoles [8], or an exact analytical expression obtained in [9]. It should be noted that the matrix elements $G_{ij}^m \equiv G^m(\boldsymbol{r}_i - \boldsymbol{r}_j)$ depend only on the vector of the difference between the centers of the cells i and j, and to calculate the demagnetization field $\boldsymbol{H}^m$, as a rule, the convolution theorem is used [10].

The basic equation describing the dynamics of a magnetic system under the influence of the static and alternating external magnetic fields is the Landau – Lifshitz nonlinear differential equation [11]

$$\frac{\partial \boldsymbol{M}_i}{\partial t} = -\gamma\left[\boldsymbol{M}_i \times \boldsymbol{H}_i^{\text{eff}}\right] - \gamma\frac{\alpha}{M_s}\boldsymbol{M}_i \times \left[\boldsymbol{M}_i \times \boldsymbol{H}_i^{\text{eff}}\right]. \tag{4}$$

Here, the first term of the right-hand side describes the precession of the magnetization of the i-th cell around the local effective magnetic field

$$\boldsymbol{H}_i^{\text{eff}}(\boldsymbol{M}_1,...,\boldsymbol{M}_N) = -\frac{1}{V_0}\frac{\delta F}{\delta \boldsymbol{M}_i} = \boldsymbol{H}_i + \sum_{j=1}^{N} G_{ij}\boldsymbol{M}_j\,, \tag{5}$$

the second term describes the damping in the system, $\gamma = 1.76\cdot10^7$ (rad/s)/Oe is the gyromagnetic ratio, and α is the damping parameter.

Using the method of successive approximations, the solution is sought in the form $\boldsymbol{M}_i = \boldsymbol{M}_{0i} + \boldsymbol{m}_i(t)$, $\boldsymbol{H}_i^{\text{eff}} = \boldsymbol{H}_{0i}^{\text{eff}} + \boldsymbol{h}_i^{\text{eff}}(t)$, where $|\boldsymbol{m}_i(t)| << |\boldsymbol{M}_{0i}|$ and $|\boldsymbol{h}_i^{\text{eff}}(t)| << |\boldsymbol{H}_{0i}^{\text{eff}}|$, $\boldsymbol{M}_{0i}$ is the equilibrium direction of the i-th magnetic moment, which in accordance with [8], is determined from a system of linear inhomogeneous equations with the undetermined Lagrange multipliers ν_i:

$$\boldsymbol{H}_{0i}^{\text{eff}}(\boldsymbol{M}_{01},\boldsymbol{M}_{02},...,\boldsymbol{M}_{0N}) = \nu_i\boldsymbol{M}_{0i}\ \ (i = 1, ..., N). \tag{6}$$

In this case, the static and dynamic parts of the effective field are determined in accordance with (5) and (6) as

$$\boldsymbol{H}_{0i}^{\text{eff}} = \sum_{j=1}^{N} G_{ij}\boldsymbol{M}_{0j} + \boldsymbol{H}_0 = \nu_i\boldsymbol{M}_{0i}, \quad \boldsymbol{h}_i^{\text{eff}}(t) = \sum_{j=1}^{N} G_{ij}\boldsymbol{m}_j(t) + \boldsymbol{h}_i^{rf}\,. \tag{7}$$

Considering only linear terms and assuming that $[\boldsymbol{M}_{0i} \times \boldsymbol{H}_{0i}^{\text{eff}}] = 0$, the equation of motion (4) takes the form [12]

$$\frac{\partial \boldsymbol{m}_i}{\partial t} = \sum_{j=1}^{N} B_{ij}\boldsymbol{m}_j + N_i\boldsymbol{h}_i^{rf}\,, \tag{8}$$

in which the following notations are used:

$$N_i = -\gamma\left(\Lambda(\boldsymbol{M}_{0i}) + \frac{\alpha}{M_s}\left(\Lambda(\boldsymbol{M}_{0i})\right)^2\right), \quad B_{ij} = N_i\left(G_{ij} - \nu_i\delta_{ij}E\right), \quad \text{and } \Lambda(\boldsymbol{M}_{0i}) \equiv \begin{pmatrix} 0 & -M_{0i}^{(z)} & M_{0i}^{(y)} \\ M_{0i}^{(z)} & 0 & -M_{0i}^{(x)} \\ -M_{0i}^{(y)} & M_{0i}^{(x)} & 0 \end{pmatrix}. \tag{9}$$

Earlier, to solve the system of equations (8), a method widely used in micromagnetic modeling was considered [13]. This method is based on finding a solution in the form of expansion in the eigenvectors of normal magnetic oscillation modes [12–16]. In this work, to reduce the required RAM capacity of the computer and the calculation time, a more efficient method was implemented, which was first used to study two-dimensional thin films with a stripe structure [17] and individual bulk ferromagnetic particles of various shapes and sizes [18, 19].

With the help of substitution $\boldsymbol{m}_i(t) = \boldsymbol{m}_{0i} e^{-i\omega t}$ and $\boldsymbol{h}_i^{rf}(t) = \boldsymbol{h}_{0i} e^{-i\omega t}$, the system of differential equations (8) is reduced to a system of linear inhomogeneous equations

$$-i\omega \boldsymbol{m}_{0i} = \sum_{j=1}^{N} B_{ij} \boldsymbol{m}_{0j} + N_i \boldsymbol{h}_{0i}. \tag{10}$$

After that, such a system can be solved by standard numerical methods of linear algebra: for example, by the iterative method of conjugate gradients or the method of minimal residuals.

It should be noted that due to the limitation $|\boldsymbol{M}_i| = M_s$, of the total number of $3N$ equations (10), only $2N$ are linearly independent, which allows reducing the number of unknowns and the calculation time. To do this, in each discrete cell, we move on to the coordinate system, the z axis of which coincides with the equilibrium direction of magnetization in it. Then, in the new coordinate system, the components of the dynamic magnetization and the alternating field will be defined as $\boldsymbol{m}'_{0i} = T_i \boldsymbol{m}_{0i}$ and $\boldsymbol{h}'_{0i} = T_i \boldsymbol{h}_{0i}$, where the transformation matrix T_i has the following form given that the azimuthal and polar angles of the vector $\boldsymbol{M}_{0i}$ are equal to φ_i and θ_i, respectively:

$$T_i = \begin{bmatrix} \cos\theta_i \cos\varphi_i & \cos\theta_i \sin\varphi_i & -\sin\theta_i \\ -\sin\varphi_i & \cos\varphi_i & 0 \\ \sin\theta_i \cos\varphi_i & \sin\theta_i \sin\varphi_i & \cos\theta_i \end{bmatrix}. \tag{11}$$

When moving to a two-dimensional problem in the new coordinate system, i.e. confining ourselves to considering only the x- and y-components of the vector and tensor quantities, we have

$$N' = N'_i = T_i N_i T_i^T = \gamma M_s \begin{bmatrix} \alpha & 1 \\ -1 & \alpha \end{bmatrix}, \; L' = (N')^{-1} = \frac{1}{\gamma M_s (1+\alpha^2)} \begin{bmatrix} \alpha & -1 \\ 1 & \alpha \end{bmatrix}. \tag{12}$$

In this case, equation (10) takes the form

$$\sum_{j=1}^{N} A'_{ij} \boldsymbol{m}'_{0j} = -\boldsymbol{h}'_{0i}, \tag{13}$$

where $A'_{ij} = G'_{ij} - \nu_i \delta_{ij} E + i\omega \delta_{ij} L'$. The solution (13) with the subsequent transition to the coordinate system associated with the simulated film by means of the inverse transformation $\boldsymbol{m}_{0i} = T_i^T \boldsymbol{m}'_{0i}$ (here, the prefix "T" means transposition) determines the solution (10).

The resulting solution describing the magnetization dynamics allows, in particular, to determine the absorption energy of the high-frequency field of the nanocrystalline TMF [20]:

$$E = \omega V_0 \sum_{i=1}^{N} \mathrm{Im}\left[\boldsymbol{m}_{0i} \boldsymbol{h}_{0i}^* \right]. \tag{14}$$

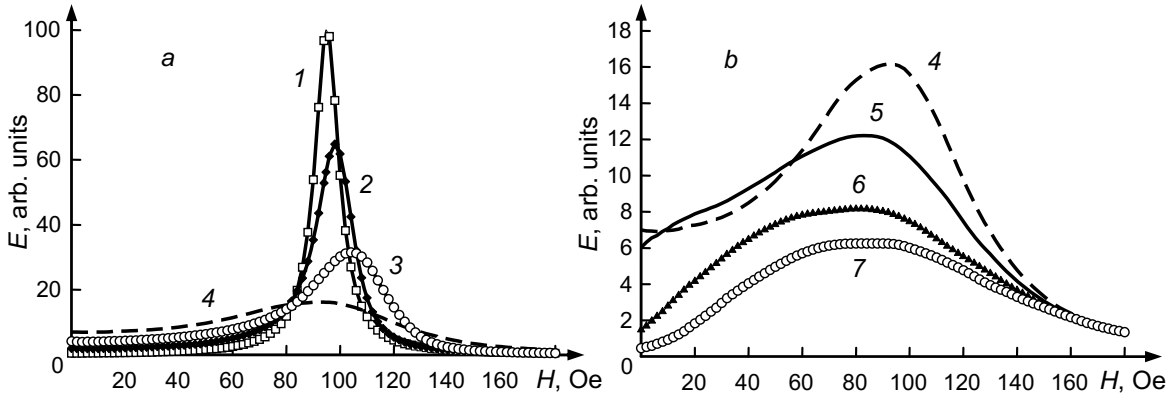

Fig. 1. Microwave absorption spectrum of a nanocrystalline thin magnetic film for various values of the crystallite size D, nm: 12 (*1*), 42 (*2*), 56 (*3*), 75 (*4*), 100 (*5*), 178 (*6*), and 1000 (*7*).

2. STUDY OF HIGH-FREQUENCY PROPERTIES OF NANOCRYSTALLINE TMF

Using the results of the calculation of the TMF micromagnetic model, a computer program was written, with the help of which the features of the microwave absorption spectra of nanocrystalline films were studied. The studies were carried out on films representing monolayers of close-packed nanoparticles with a random distribution of the anisotropy axes. The numbers of particles were 128×128×1. The size of nanoparticles D corresponded to the size of discrete cells in the model and varied within 12–1000 nm. To eliminate the edge effects associated with the inhomogeneity of the internal magnetic field near the sample boundaries, we used two-dimensional infinite periodic boundary conditions for calculating the exchange and magnetostatic interaction energies [21]. For definiteness, the magnetic parameters of the samples under study were chosen in accordance with the well known nanocrystalline alloy $Fe_{73.5}Cu_1Nb_3Si_{13.5}B_9$ [7], the saturation magnetization of which is M_s = 955 G (1.2 T), the exchange constant $A = 1\cdot10^{-6}$ erg/cm ($1\cdot10^{-11}$ J/m), the local uniaxial anisotropy field is $H_k = 2K/M_s$ = 171.7 Oe (K = 8200 J/m^3), and the damping parameter is α = 0.005. In this case, the magnetic anisotropy K_u common for the entire film was not taken into account. The external static magnetic field was applied in the film plane and ranged within 0–180 Oe, and the in-plane alternating magnetic field with a pump frequency f = 3 GHz was directed orthogonally to the static field. It is important to note that an analytical expression was used to calculate the components of tensor of the magnetostatic interaction between crystallites [9].

Figure 1 shows the results of the calculation of the microwave absorption spectra of nanocrystalline TMFs for some values of D. Curves *1–4* in Fig. 1*a* correspond to the resonance absorption lines for films with the crystallite sizes D = 12, 42, 56, and 75 nm, and curves *4–7* in Fig. 1*b* correspond to the FMR lines for the films with D = 75, 100, 178, and 1000 nm. It can be seen that the crystallite size of TMF has a strong influence on the shape and position of the resonance curve, and this effect, as shown by studies, is particularly significant for films, in which the crystallite size is in a certain "critical" range starting with a size $D \sim 35$ nm, at which the random magnetic anisotropy energy $F^a = -VK$ is equal to the exchange energy $F^e = -VJ$.

An analysis of the curves shows that an increase in the crystallite size leads to a change in the FMR field, a significant broadening of the resonance absorption line, and also the appearance of an asymmetry in the shape of the resonance curve. Note that for a film with the minimum crystallite size (D = 12 nm), the exchange energy is more than 8 times higher than the uniaxial random magnetic anisotropy energy, the shape of its resonance curve is close to the symmetric one, and the resonance field H_R and the FMR line width ΔH_R almost coincide with the resonance field $H_0 \approx \pi\,(f/\gamma)^2/M_s \sim 95$ Oe and the FMR line width $\Delta H_0 \approx 4\pi\alpha f/\gamma \sim 10.7$ Oe obtained for an isotropic uniformly magnetized TMF. However, for a film with D = 100 nm, in which the exchange energy, on the contrary, is more than 8 times less than the random magnetic anisotropy energy, the resonance field is shifted by $\delta H = H_R - H_0$ equal to ~–12 Oe and the FMR line broadens by the value $\delta\Delta H = \Delta H_R - \Delta H_0$ equal to ~120 Oe. At the same time, the

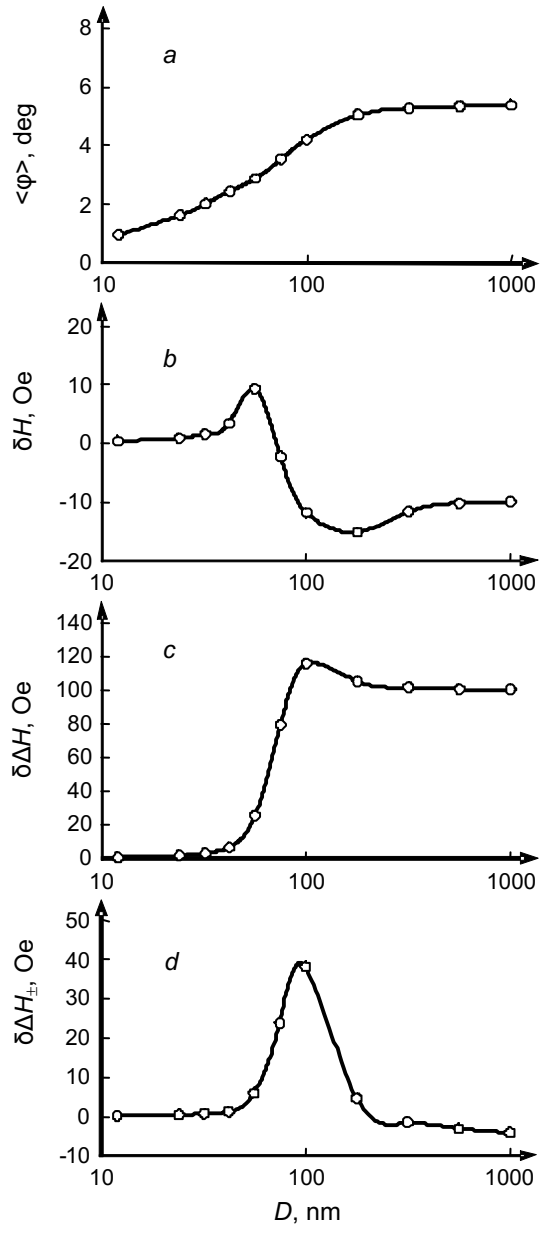

Fig. 2. Dependence of the root-mean-square deviation of the inhomogeneous magnetization angle on the average direction (*a*), resonance displacement (*b*), broadening (*c*), and asymmetry of the resonance line (*d*) on the size of the TMF crystallites.

asymmetry of the resonance line shape $\delta\Delta H_{\pm}$ defined as the difference between the left ΔH_{-} and right ΔH_{+} "half-widths" of the FMR line ($\delta\Delta H_{\pm} = \Delta H_{-} - \Delta H_{+}$) is ~ 40 Oe for the film with D = 100 nm. It should be noted that to calculate the values of H_R, ΔH_R, ΔH_{-}, and ΔH_{+}, we used the approximation of the microwave absorption spectra obtained using the so-called asymmetric Lorenz resonance curve proposed in [22].

Figure 2*a* shows the dependence of the root-mean-square deviation of the inhomogeneous magnetization angle <φ> of a nanocrystalline film on the average direction of the magnetization in TMF constructed for various values of the crystallite sizes. The values of <φ> characterizing the state of the magnetic microstructure of the film were obtained for the external static magnetic field equal to the resonance field $H = H_R$. It can be seen from the figure that with

increasing D, a monotonic, almost linear increase in the root-mean-square deviation $\langle\varphi\rangle$ is observed up to $D \sim 150$ nm in the "critical" range. For $D > 180$ nm, $\langle\varphi\rangle$ remains almost constant.

In contrast to this behavior of $\langle\varphi\rangle$ (D), the dependences of the resonance field shift $\delta H(D)$ (Fig. 2*b*), the broadening of the FMR line $\delta\Delta H(D)$ (Fig. 2*c*), and the asymmetry of the resonance curve $\delta\Delta H_{\pm}(D)$ (Fig. 2*d*) have a pronounced non-monotonous character. Thus, the shift of the resonance field δH first increases with increasing crystallite size, reaching its maximum $\delta H \sim 10$ Oe at $D \sim 56$ nm, then, at $D \sim 75$ nm, the shift of the FMR field changes the sign to the opposite one, reaching a minimum of $\delta H \sim -15$ Oe at $D \sim 180$ nm, and in the range of $D \sim 300$–1000 nm, the shift reaches the saturation $\delta H \sim -10$ Oe.

The dependence of the broadening of the FMR line (Fig. 2c) increases in the "critical" range of the crystallite sizes, demonstrating a sharp, almost linear increase in $\delta\Delta H$ in the range $D \sim 40$–90 nm and reaching a maximum at $D \sim 100$ nm. The line width $\Delta H_R \sim 130$ Oe at this point is an order of magnitude larger than the width ΔH_0 of the FMR line of an isotropic magnetic film with a uniform structure. With a further increase in the crystallite size, $\delta\Delta H$ slightly decreases and at $D > 300$ nm, it reaches saturation $\delta\Delta H \sim 100$ Oe.

The behavior of the dependence $\delta\Delta H_{\pm}(D)$ characterizing the asymmetry of the FMR line shape is interesting (Fig. 2*d*). In the range $D \sim 40$–90 nm, it behaves similarly to the dependence $\delta\Delta H$ (D) demonstrating a sharp increase and also reaches its maximum at $D \sim 100$ nm. However, then, it rapidly decreases to zero at $D \sim 200$ nm (in this case, the FMR line becomes symmetric), and then, it changes the sign and decreases monotonically. In other words, for small sizes of crystallites in TMF, the steepness of the left slope of its resonance curve is less than that of the right slope, and for large sizes of crystallites, vice versa.

CONCLUSIONS

Thus, to study high-frequency properties of nanocrystalline magnetic films, a micromagnetic model has been developed that takes into account the random distribution of the uniaxial magnetic anisotropy directions in crystallites. In addition to the Zeeman energy and energy of uniaxial magnetic anisotropy, the model takes into account the energies of the exchange and magnetic dipole (magnetostatic) interaction of magnetic moments. On the basis of this model, an effective method has been implemented for numerical analysis of the magnetization dynamics of nanocrystalline films in microwave fields, which made it possible to significantly reduce the RAM capacity of the computer and also significantly reduce the calculation time.

The performed studies allowed us to find features in the ferromagnetic resonance spectra associated with the influence of the crystallite sizes D on the parameters of the resonance curve. In particular, it was found that in a certain "critical" range of the crystallite sizes, where the energy of random magnetic anisotropy begins to exceed the exchange energy, a significant change in the ferromagnetic resonance field, a multiple increase in the width of the resonance line, and the appearance of a resonance curve asymmetry are observed. It is shown that with an increase in the crystallite size, the resonance field first grows, reaching a maximum, then, it rapidly decreases to its minimum, and then, it grows again to reach saturation. In this case, the steepness of the left slope of the broadening resonance curve first decreases faster than that of the right slope, leading to the symmetry breaking of the resonance curve shape, and then, the curve becomes symmetrical again, and the steepness of the left slope becomes greater than that of the right slope.

The conducted studies are, firstly, of great importance for the physics of magnetic phenomena, since the detection of new effects always makes it possible to better understand the nature of the observed features in the microwave absorption spectra of ferromagnetic materials. Secondly, the results obtained in this work are of great interest for technologists working on the problem of creating nanocrystalline magnetic films with given high-frequency properties.

This work was supported by the Ministry of Education and Science of the Russian Federation, project No. RFMEFI60417X0179.

REFERENCES

1. J. Petzold, JMMM, **242–245**, 84–89 (2002).
2. M. Yamaguchi, K. H. Kim, and S. Ikedaa, JMMM, **304**, 208–213 (2006).
3. A. N. Babitskii, B. A. Belyaev, N. M. Boev, *et al*., Instruments and Experimental Techniques, **59**, No. 3, 425–432 (**2016**).
4. B. A. Belyaev, N. M. Boev, A. V. Izotov, *et al*., Russ. Phys. J., **61**, No. 8, 1367–1375 (2018).
5. A. N. Lagar'kov, S. A. Maklakov, *et al*., J. Commun. Technol. Electron., **54**, No. 5, 596–603 (2009).
6. O. Acher and A. L. Adenot, Phys. Rev. B, **62**, 11324–11327 (2000).
7. G. Herzer, JMMM, **157/158**, 133–136 (1996).
8. B. A. Belyaev, A. V. Izotov, and An. A. Leksikov, Phys. Solid State, **52,** No. 8, 1664–1672 (2010).
9. A. J. Newell, W. Williams, and D. J. Dunlop, J. Geophys. Res., **98**, 9551–9555 (1993).
10. B. Van de Wiele, F. Olyslager, L. Dupre´, and D. De Zutter, JMMM, **322**, 469–476 (2010).
11. A. G. Gurevich, Magnetic Resonance in Ferrites and Antiferromagnets [in Russian], Nauka, Moscow (1973).
12. B. A. Belyaev and A. V. Izotov, Phys. Solid State, **55,** No. 12, 2491–2500 (2013).
13. A. V. Izotov and B. A. Belyaev, Russ. Phys. J., **53**, No. 9, 900–905 (2011).
14. M. Grimsditch, L. Giovannini, F. Monotcello, *et al*., Phys. Rev. B, **70**, 054409 (2004).
15. K. Rivkin and J. B. Ketterson, JMMM, **306**, 204–210 (2006).
16. M. D'aquino, C. Serpico, G. Miano, and C. Forestiere, J. Comput. Phys., **228**, 6130–6149 (2009).
17. N. Vukadinovic, O. Vacus, M. Labrune, *et al*., Phys. Rev. Lett., **85**, 2817–2820 (2000).
18. S. Labbe and P.-Y. Bertin, JMMM, **206**, 93–105 (1999).
19. C. Vaast-Paci and L. Leylekian, JMMM, **237**, 342–361 (2001).
20. L. D. Landau and E. M. Lifshits, Electrodynamics of Continuous Media, 2-nd ed. [in Russian], Nauka, Moscow (1982).
21. K. M. Lebecki, M. J. Donahue, and M. W. Gutowski, J. Phys. D: Appl. Phys., **41**, 175005 (2008).
22. A. L. Stancik and E. B. Brauns, Vibrational Spectrosc., **47**, 66–69 (2008).